 CMES, vol.27, no.2, pp.111-123, 2008

A Micromechanical Model for Polycrystal Ferroelectrics with Grain Boundary Effects

K. Jayabal, A. Arockiarajan and S.M. Sivakumar [1]

Abstract: A three dimensional micromechanically motivated model is proposed here based on firm thermodynamics principles to capture the nonlinear dissipative effects in the polycrystal ferroelectrics. The constraint imposed by the surrounding grains on a subgrain at its boundary during domain switching is modeled by a suitable modification of the switching threshold in a subgrain. The effect of this modification in the dissipation threshold is studied in the polycrystal behavior after due correlation of the subgrain behavior with the single crystal experimental results found in literature. Taking into consideration, all the domain switching possibilities, the volume fractions of each of the variants in a sub-grain is tracked and homogenized for polycrystal behavior. The results show appreciable improvement in modeling the response of the polycrystal ferroelectrics under electromechanical loading conditions.

Keyword: Ferroelectrics, domain switching, micromechanical modeling, boundary effects

1 Introduction

Ferroelectrics are materials that behave like piezoelectric materials under low electrical and mechanical loads and undergo a unique phenomenon called domain switching under higher loads. The various functional applications of the ferroelectrics due to their electromechanical coupling behavior include sensors, actuators, and MEMS devices. In general, all these devices function within the linear coupling limit forcing the device designers to work within a small region of a greater potential. In addition, present day devices have complex geometries upon demand from the device design. When subjected to severe electromechanical loading, they develop concentrations of electric and mechanical field within their domain. This causes the material to undergo domain switching and associated nonlinearity that may affect the performance of the ferroelectric devices. Hence, developing a nonlinear constitutive model that will characterize the material behavior in a better way can address the above problems and improve the design of devices.

Ferroelectric constitutive models can be, in general, classified as phenomenological models and micromechanical models. Phenomenological models are commonly derived from a thermodynamic framework and use evolving functions that need a lot of curve fitting based on experimental observations (Cocks and McMeeking (1999); Kamlah and Jiang (1999); Landis and McMeeking (2000); McMeeking and Landis (2002); Shieh, Huber, and Fleck (2003)). These models give a purely phenomenological picture, and do not describe the microstructural changes that accompany the processes of polarization and switching from a physical angle. The development of phenomenological models, their formulations and recent advances, and, their applications are in detail reported by Kamlah (2001); Landis (2004). Micromechanical models are based on a description of the material at the domain or single crystal level and a homogenization is applied to reproduce the polycrystal behavior. The increasing need for numerical constitutive experiments with complex electromechanical loading histories, difficult to conduct in lab, demands the use of micromechanical models to fix the trends. Nowadays, micromechanical models are applied to design and development of piezoelectric transducers of small length scales and in thin film de-

[1] Department of Applied Mechanics, Indian Institute of Technology Madras, 600036 Chennai, India

vices.

A detailed review on recent developments on micromechanical models is discussed by Huber (2005). A domain switching micromechanical model was proposed that assumes that each grain contains a single domain and the switching occurs instantly as the critical energy criterion is met (Hwang, Lynch, and McMeeking (1995)). Later modifications were done to simplify or to broaden the applicability of these models (Michelitsch and Kreher (1998); Lu, Fang, Li, and Hwang (1999)). Nevertheless, these models do not consider the interaction effects due to the surrounding crystallites and the presence of distinct domains in each grain at a given time. The interaction effect is taken into the switching criterion by modifying the loads (Chen and Lynch (1998); Hwang, Huber, McMeeking, and Fleck (1998)) or using self consistent homogenization methods by appropriate averaging of the grain responses (Huber, Fleck, Landis, and McMeeking (1999)). Many finite element based models were developed in the past and recently, a three dimensional finite element based micromechanical model was proposed to capture the nonlinear behavior of ferroelectrics, wherein the grain boundary effects are incorporated via a macromechanically motivated probabilistic approach and via element to element displacement continuity constraints (Arockiarajan, Menzel, Delibas, and Seemann (2006); Arockiarajan and Menzel (2007)). In order to truly capture the meanfield effects, the number of elements considered is to be very large and certain periodic boundary conditions are to be assumed. To avoid such difficulties and the complexity of using Eshelby inclusion models, we consider in this work the interaction effects due to grain boundary in a simple way that is directly brought into the formulation. For simplicity, Reuss approximation, where the stress and electric field are considered to be uniform throughout the material, is used to obtain the macroscopic response by averaging microscopic responses. The advantage is immense considering that the computational effort is drastically reduced in this exercise. Also, flexibility exists in terms of adjusting these variables that are to be determined phenomenologically using experimental observations. Obtaining a reasonably good expression to indicate when the domain switching takes place in ferroelectrics is a significant task in micromechanical modeling. Various energy criteria for domain switching have been proposed in the past based on total work done (Hwang, Lynch, and McMeeking (1995); Sun and Jiang (1998)), Gibbs energy (Lu, Fang, Li, and Hwang (1999)), total potential (Hwang and McMeeking (2000)), and internal energy density (Sun and Achuthan (2001)). An energy criterion, utilizing both Gibbs energy and internal energy, assigning importance to loading sequence, was also proposed earlier after testing switch-worthiness (Shaikh, Phanish, and Sivakumar (2006)). Simple and elegant micromechanical models with more physical insight brought into it, which can predict the response of polycrystal well, are the need of the hour.

The work presented here deals with a thermodynamically consistent micromechanical model using a new domain switching criterion that includes pressure dependent boundary effects. The paper highlights the following that form the main features of the work:

- A thermodynamically consistent, dissipation maximization based formulation that considers domain switching under electromechanical loading conditions is proposed and formulated.
- A crystallographic theory has been used to obtain the domain switching criterion that is consistent with compatibility at the variant interfaces.
- The boundary effects are incorporated by a suitable modification of the switching threshold function at the subgrain level. This is initially verified for a constrained single crystal and later used in the simulation of a polycrystal ferroelectric.

The results show appreciable improvement in modeling the response of the polycrystal ferro-

electrics under electromechanical loading conditions.

2 Theoretical preliminaries

2.1 Electrostatics and thermodynamics

In this section, the governing field equations relevant for the behavior of ferroelectrics are discussed. This includes static mechanical equilibrium, static electrical equilibrium, kinematic relations, and first and second law of thermodynamics.

For a ferroelectric body in static mechanical equilibrium, the stress $\boldsymbol{\sigma}$ is in balance with the external body forces $\vec{b}$ satisfying the following equation:

$$\nabla \cdot \boldsymbol{\sigma} + \rho \vec{b} = 0. \tag{1}$$

Similarly, for electric equilibrium, the electric displacement $\vec{D}$ is in balance with the external electric charge q through,

$$\nabla \cdot \vec{D} - q = 0. \tag{2}$$

Considering quasi-static conditions, electric field $\vec{E}$ and electric potential ϕ are related through,

$$\vec{E} = -\nabla \phi \tag{3}$$

and on the surface of the body, the stress and traction $\vec{T}$ are related through the unit outward normal $\vec{n}$ by,

$$\vec{T} = \boldsymbol{\sigma} \cdot \vec{n} \tag{4}$$

In this work, we assume that the strain is sufficiently small so that we can apply infinitesimal theory, with the total strain derived from displacement field $\vec{u}$ as

$$\boldsymbol{\varepsilon}_{ij} = \frac{1}{2}\left(u_{i,j} + u_{j,i}\right). \tag{5}$$

To lay the ground for developing the constitutive description for multi domain crystallite, we recall the first and second laws of thermodynamics for deformable dielectric materials.

$$\rho \dot{U} = \boldsymbol{\sigma} : \dot{\boldsymbol{\varepsilon}} + \vec{E} \cdot \dot{\vec{D}} - \nabla \cdot \vec{q} \tag{6}$$

$$\rho \dot{\eta} - \nabla \cdot \left(\frac{\vec{q}}{\theta}\right) \geq 0 \tag{7}$$

where, U denotes internal energy density, $\boldsymbol{\sigma}$, applied stress tensor, $\boldsymbol{\varepsilon}$, total strain tensor, $\vec{E}$, applied electric field, η, entropy density, $\vec{q}$, heat flux, and θ, absolute temperature of the material, respectively. A superscribed dot indicates the time derivatives of that particular quantity. Using the Legendre transform, Gibbs energy G can be expressed as

$$G = u - \boldsymbol{\sigma} : \boldsymbol{\varepsilon} - \vec{E} \cdot \vec{D} - \eta\theta \tag{8}$$

2.2 Ferroelectrics

Here, we discuss a few points, related to the physics involved in the microstructure of ferroelectrics that will form the basis for developing the proposed model. A ferroelectric ceramic contains many grains and each grain consists of many domains that are a group of unit cells, oriented in a particular direction determined by the crystallographic structure of the material. Each unit cell exhibits polarization and an associated strain with respect to the reference state defined above Curie temperature and these are called spontaneous strain and spontaneous polarization. In a depoled state, the ferroelectrics do not have a net strain and net polarization since the domains are randomly oriented in the material true to its configurationally maximum entropic state.

On application of external loads, either electrical or mechanical, initially, the ferroelectric unit cell undergoes a recoverable change in polarization and strain in the same domain type. When the loads exceed a certain limit, the unit cell may reorient its polarization direction itself that is favorable to the external loads. This change in domain type in ferroelectrics is referred as domain switching and is irrecoverable in nature. As the external loads increases, a specific domain type is favored at the expense of others. Domain switching may originate at a boundary, in general on the surface, and progress inside or it may nucleate at various regions in the material and move toward each other. The sharp interface that separates distinct domains is called domain wall. At any instant, a specific domain type in a crystal can be

represented by its volume fraction, which is considered as an internal variable in micromechanical models. A domain type can be represented by a unit cell that it belongs to.

In paraelectric state, above Curie temperature, the unit cell assumes a cubic structure and in ferroelectric state, below Curie temperature, the unit cell may assume other crystal structures like tetragonal, rhombohedral, depending upon the composition of ferroelectrics. Here, we confine our discussion to a tetragonal structure though the concept can be conveniently extended to any other crystal structure. Spontaneous strain of a unit cell with its polarization along x_3 direction can be expressed in terms of its lattice parameters as

$$\boldsymbol{\varepsilon}_i = \begin{bmatrix} \frac{a-a_0}{a_0} & 0 & 0 \\ 0 & \frac{a-a_0}{a_0} & 0 \\ 0 & 0 & \frac{c-a_0}{a_0} \end{bmatrix} \tag{9}$$

while a_0 defines the cubic structure in paraelectric phase, a and c define the tetragonal structure in ferroelectric phase.

The total strain and electric displacement of a unit cell can be assumed to be decomposable as a recoverable part with a subscript r and an irrecoverable part with a subscript i as

$$\boldsymbol{\varepsilon} = \boldsymbol{\varepsilon}_r + \boldsymbol{\varepsilon}_i \tag{10}$$

$$\vec{D} = \vec{D}_r + \vec{D}_i \tag{11}$$

The volume fraction of a domain type α, ξ^α, will have to satisfy the following conditions for a tetragonal perovskite material consisting of six distinct domains,

$$\xi^\alpha \geq 0 \;\; ; \;\; \sum_{\alpha=1}^{6} \xi^\alpha = 1 \;\; \& \;\; \sum_{\alpha=1}^{6} \dot{\xi}^\alpha = 0. \tag{12}$$

The total strain and total electric displacement of the crystal can be obtained in terms of volume fractions as,

$$\boldsymbol{\varepsilon} = \sum_{\alpha=1}^{6} \boldsymbol{\varepsilon}^\alpha \xi^\alpha \tag{13}$$

$$\vec{D} = \sum_{\alpha=1}^{6} \vec{D}^\alpha \xi^\alpha \tag{14}$$

Similarly, Gibbs energy for the total crystallite, assuming that the interface contributions are negligible compared to that of bulk, can be obtained by the sum of individual domains,

$$G(\boldsymbol{\sigma}, \vec{E}, \theta, \xi^\alpha) = \sum_{\alpha=1}^{6} \xi^\alpha G^\alpha \tag{15}$$

Assuming isothermal processes and homogeneous temperature fields, the heat flux term can be eliminated and the resulting dissipation inequality can be derived using eqs.((6) to (8) and (10) to (15)),

$$\begin{aligned} -\left[\rho \frac{\partial G}{\partial \boldsymbol{\sigma}} + \sum_{\alpha=1}^{6} \boldsymbol{\varepsilon}_r^\alpha\right] \dot{\boldsymbol{\sigma}} - \left[\rho \frac{\partial G}{\partial \vec{E}} + \sum_{\alpha=1}^{6} \vec{D}_r^\alpha\right] \dot{\vec{E}} \\ + \sum_{\alpha=1}^{6} \left[\boldsymbol{\sigma} : \Delta\dot{\boldsymbol{\varepsilon}}_i^\alpha + \vec{E} \cdot \Delta\dot{\vec{D}}_i^\alpha\right] \\ - \sum_{\alpha=1}^{6} \left[\rho \frac{\partial G}{\partial \xi^\alpha}\right] \dot{\xi}^\alpha \geq 0 \end{aligned} \tag{16}$$

where $\Delta\dot{\boldsymbol{\varepsilon}}^\alpha$ and $\Delta\dot{\vec{D}}^\alpha$ represent respectively, the rate at which the change in spontaneous strain and spontaneous polarization occurs in favor of α type domains from any other domains.

$$\Delta\dot{\boldsymbol{\varepsilon}}_i^\alpha = \sum_{\beta=1}^{6} \Delta\boldsymbol{\varepsilon}_i^{\beta\to\alpha} \dot{\xi}^{\beta\to\alpha} \;\; ; \;\; \alpha \neq \beta \tag{17}$$

$$\Delta\dot{\vec{D}}_i^\alpha = \sum_{\beta=1}^{6} \Delta\vec{D}_i^{\beta\to\alpha} \dot{\xi}^{\beta\to\alpha} \;\; ; \;\; \alpha \neq \beta \tag{18}$$

and,

$$\dot{\xi}^\alpha = \sum_{\beta=1}^{6} \dot{\xi}^{\beta\to\alpha} \;\; ; \;\; \alpha \neq \beta \tag{19}$$

where,

$$\Delta\boldsymbol{\varepsilon}_i^{\beta\to\alpha} = \boldsymbol{\varepsilon}_i^\alpha - \boldsymbol{\varepsilon}_i^\beta \tag{20}$$

$$\Delta\vec{D}_i^{\beta\to\alpha} = \vec{D}_i^\alpha - \vec{D}_i^\beta \tag{21}$$

Applying enforced conditions on controllable state variables $\boldsymbol{\sigma}$ and $\vec{E}$ in eq.(16), and using

eqs.((17),(18), and (19)), the dissipation potential for the material is obtained as

$$\sum_{\alpha=1}^{6}\sum_{\beta=1}^{6}\left(\boldsymbol{\sigma}:\Delta\boldsymbol{\varepsilon}_i^{\beta\to\alpha}+\vec{E}\cdot\Delta\vec{D}_i^{\beta\to\alpha}-\rho\frac{\partial G}{\partial\xi^{\beta\to\alpha}}\right)\cdot\dot{\xi}^{\beta\to\alpha}\geq 0\,;\quad \alpha\neq\beta \tag{22}$$

which is the product of driving force, (shown within the parenthesis in the above equation), and the rate at which the volume fraction of a particular domain type evolves. The above inequality is valid subject to the constraints given in eq.(12). The first two terms in the driving force appearing in eq.(22) concern the external stress and electric fields while the third term concerns the driving forces attributed to domain to domain interactions at the subgrain level and grain to grain interactions at the polycrystal level.

As mentioned earlier, there exist six different types of domains in a tetragonal perovskite structure. Externally applied loads, on reaching a critical value, induce domain switching among various domains. Referring a transformation system to each domain switching process involving two different domains, it becomes clear from eq.(22) that there are as many as 30 transformation systems possible (in this, $\beta\to\alpha$ switching is taken to be different from $\alpha\to\beta$). For clarity, let us suppose that there exist only two types of domains α and β in the crystal at a given time and the recoverable Gibb's energy of the crystal can be expressed as

$$G=\xi^{\alpha}G^{\alpha}+\xi^{\beta}G^{\beta}=G^{\beta}+\Delta G_{\alpha-\beta}\xi^{\alpha} \tag{23}$$

where

$$\begin{aligned}\Delta G_{\alpha-\beta}=&G_{\alpha}-G_{\beta}\\ =&-\frac{1}{2}\boldsymbol{\sigma}:\left(\boldsymbol{C}^{\alpha}-\boldsymbol{C}^{\beta}\right):\boldsymbol{\sigma}\\ &-\frac{1}{2}\vec{E}\cdot\left(\boldsymbol{\kappa}^{\alpha}-\boldsymbol{\kappa}^{\beta}\right)\cdot\vec{E}\\ &-\vec{E}\cdot\left(\boldsymbol{d}^{\alpha}-\boldsymbol{d}^{\beta}\right):\boldsymbol{\sigma}\end{aligned} \tag{24}$$

The above expression eq.(24) can be used to obtain the third term of the driving force in the eq.(22). Here, ξ^{α} and ξ^{β} refer to the volume fractions of domains α and β respectively. In arriving second part of eq.(23), the constraint $\xi^{\alpha}+\xi^{\beta}=1$ is used. Also, $\boldsymbol{C}$ denotes the compliance tensor, $\boldsymbol{\kappa}$, the dielectric susceptibility tensor, and $\boldsymbol{d}$, the piezoelectric tensor. Let the external loading induces domain switching that transforms domains from β type to α type. The dissipation potential for this transformation from eq.(22),

$$F_{drive}\dot{\xi}^{\alpha}\geq 0 \tag{25}$$

where

$$F_{drive}=\boldsymbol{\sigma}:\Delta\boldsymbol{\varepsilon}_i+\vec{E}\cdot\Delta\vec{D}_i-\Delta G_{\alpha-\beta} \tag{26}$$

For the transformation system considered above to be active, i.e., for domains to start switching from β type to α type in the crystal, during the impending material energy dissipation, the driving force in eq.(26) must satisfy the following inequality at all times:

$$F_{drive}\dot{\xi}^{\alpha}\leq F_c\dot{\xi}^{\alpha} \tag{27}$$

where, F_c denotes a critical value, the driving force should attain for domain switching. It is assumed here that the transformation is stable, i.e. the rate of resistance to transformation is higher than the rate of driving force. In general, we don't know a priori whether switching will take place from β to α or vice versa. Hence, the driving force for both the transformation systems are calculated separately for the given loading and multiplied with the corresponding volume fraction rates. It is to be noted, here, that the rates of volume fractions are assumed to be positive in both the transformations, and, hence, the switching process is decided strictly by driving forces.

3 Switching criterion

After deriving the driving force for transformation systems, we proceed further to obtain the critical value for driving force in order to check for domain switching. Many switching criteria have been developed in the past, incorporating work done, Gibb's energy, total potential and internal energy density. A new criterion is proposed in this model for 90^0 switching, drawing analogy from plasticity on the fact that the resolved shear stress determines yielding.

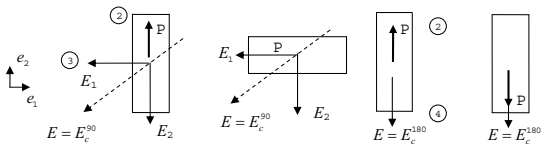

(a) (b) (c) (d)

Figure 1: 90^0 domain switching (a) and (b), and 180^0 domain switching (c) and (d).

A domain can undertake an 180^0 switching (Fig.1.(c) and (d)) or any of four 90^0 switching (Fig.1.(a) and (b)) due to externally applied loads. Since the underlying mechanism for 90^0 switching and 180^0 switching are different, the critical values for their occurrence are also different. Domains are randomly scattered in ferroelectric polycrystals, and the external electric field act on them along different angles with respect to the crystal axes depending upon their orientation. It is assumed, here, that 90^0 domain switching takes place in ferroelectrics in the same way, the yielding occurs in materials. Hence, when the applied electric field reaches the coercive electric field in a unit cell on a critical plane that is oriented at an angle of 45^0 with the polarization direction, 90^0 domain switching occurs. For instance, consider a domain that is oriented along positive e_2 direction that is named as domain type 2 (Fig.1.(a)). It has four critical planes with respect to 90^0 switching and they are aligned towards positive and negative directions of e_1 and e_3. The magnitude of increasing electric field is resolved on these four planes and when it reaches the coercive field in any of these planes, 90^0 switching occurs towards that plane. Let us suppose that the electric field induces switching from domain type 2 to domain type 3, which is oriented in the negative e_1 direction. Using eqs.(25) and (26), the driving force for 90^0 switching can be obtained as,

$$F_c^{90} = \vec{E} \cdot (\vec{P}_0^3 - \vec{P}_0^2) + \frac{1}{2}\vec{E} \cdot (\boldsymbol{\kappa}^3 - \boldsymbol{\kappa}^2) \cdot \vec{E} \qquad (28)$$

$$F_c^{90} = \sqrt{2} E_c^{90} P_0 \qquad (29)$$

Here, E_c^{90} refers to the magnitude of coercive electric field for 90^0 switching and, P_0, the magnitude of the spontaneous polarization. $\vec{P}_0^2$ and $\vec{P}_0^3$ represent the spontaneous polarization vectors and, $\boldsymbol{\kappa}^2$ and $\boldsymbol{\kappa}^3$ represent the dielectric permittivity tensors for domain types 2 and 3 respectively. Polarization and electric displacements are interchangeably used for materials with high dielectric constants. When the applied electric field in the opposite direction of polarization reaches the coercive electric field, 180^0 switching occurs. For instance, consider the switching from domain type 2 to domain type 4 (Fig.1.(c) and (d)). From eqs.(25) and (26), the driving force for 180^0 switching can be obtained as,

$$F_c^{180} = \vec{E} \cdot (\vec{P}_0^4 - \vec{P}_0^2) + \frac{1}{2}\vec{E} \cdot (\boldsymbol{\kappa}^4 - \boldsymbol{\kappa}^2) \cdot \vec{E} \qquad (30)$$

$$F_c^{180} = 2 E_c^{180} P_0 \qquad (31)$$

It is to be noted that the coercive electric field for 180^0 switching, E_c^{180}, is different from that of 90^0 switching, E_c^{90}. Eqs.(29) and (31) give the expressions for critical values that should be overcome by the driving forces to induce domain switching without considering grain boundary effects. However, these effects are to be included in the model in order to predict the material response in a more realistic way. To include the crystal boundary effects in the model, the critical values are modified appropriately in the following section.

4 Grain boundary effects

A ferroelectric single crystal in a depoled state may possess all different types of domains possible and, with external load, all domains can be transformed into a single domain type. Since there are no grain boundaries inside a single crystal, domains experience negligible resistance (that arise from domain-domain interfaces), while switching. But in polycrystals, there exist a number of grains and each of them is separated from the others by grain boundaries. Grain boundaries are generated in the crystal due to variation in the crystallographic orientations of unit cells in grains. The presence of these crystal boundaries may resist the motion of the interface between the original and the switched domains during domain switching under an external loading condition. This increases the driving force necessary

for the progress of switching. During the progress of switching, some part of the resistance goes towards the increased stored energy while some part of it is dissipated.

The dissipative part of the resistance to overcome the grain boundary constraints by a switching subgrain in a ferroelectric polycrystal is taken to be a function of the applied stress in addition to the threshold discussed in the previous section. Thus, this resistance experienced by the driving force due to the presence of the neighboring grains in a polycrystal during a 90^0 switching is, thus, taken to be,

$$F^{90}_{drive} = F^{90}_c + K_2 < -\sigma > \xi^\alpha \tag{32}$$

Here, ξ^α denotes the volume fraction of a domain at a given state, while incremental switching takes place in favor of α domain from other domains. It should be pointed out that the stress considered here is always compressive in nature and σ represents the compressive applied pressure (the trace of the applied stress). A positive $\boldsymbol{\sigma}$ is assumed to have no effect as is expressed in the above equation using a Macaulay bracket, $< \cdot >$ which is zero when $\cdot$ is negative. Therefore, second expression on the right hand side of eq.(32) is taken to be zero when $\boldsymbol{\sigma}$ is positive. K_2 is a material constant that is determined from experiments. The stored energy part of the grain boundary interaction forms a part of the driving force given in equation (22). Specifically, an additional term, $K_1\xi^\alpha$ is introduced into the third term of driving force expression in equation (22) that concerns grain to grain interactions. K_1 is a material constant that is determined from experiments. An assumption that the boundary effects during 180^0 switching, does not play a major role in additional dissipation and thus, the driving force can be expressed, as in eq.(31), as

$$F^{180}_{drive} = F^{180}_c \tag{33}$$

5 Simulation procedure

In this model, a grain containing all distinct types of domains with equal probability at the beginning is considered for simulations. Hence, initially, the net strain and polarization of the grain is zero, because the spontaneous strain and spontaneous polarization of individual domains in the grain will cancel each other on averaging. Two types of coordinate systems are used in the simulation to refer to the material properties and external loadings; one is the global coordinate system with respect to the bulk material and the other is a local coordinate system with respect to the individual grains. These two coordinate systems are related through a rotation tensor, $\boldsymbol{R}$, through

$$\underline{\vec{e}} = \boldsymbol{R} \cdot \vec{e} \tag{34}$$

where, $\underline{\vec{e}}$ and $\vec{e}$ are the base vectors of local and global coordinate systems respectively. Local coordinate system representing the grain orientation is generated using Euler angles and the domain type 1 is assumed to align with x_3 axis of the coordinate system. The other five domains are positioned in the local coordinate system with respect to domain type 1. Once the local coordinate system is generated in space for a grain, then, it is considered to be fixed with respect to that grain as it does not change with domain switching. The elastic, dielectric and piezoelectric properties of other domains are obtained by transforming the material properties of domain 1 using transformation law. The macroscopic response of the material is obtained by averaging the microscopic responses of individual grains. Since the intergranular effects are included within the switching criterion, a simple Reuss approximation is found sufficient for averaging purposes. Under Reuss approximation, the electric and stress fields are uniform inside the material and they equal the external applied fields.

The external electromechanical loading given in the global coordinate system is resolved and applied to each grain, in its respective local coordinate system. The response of all domains in that grain is determined using eq.(32) and (33) under the given loading. The strain, $\boldsymbol{\varepsilon}^g$, and the polarization, $\vec{P}^g$, of each grain is obtained by summing up the total strain and total polarization of individual domains within the grain.

$$\boldsymbol{\varepsilon}^g = \sum_{\alpha=1}^{6} (\boldsymbol{\varepsilon}^\alpha_i + \boldsymbol{C}^\alpha : \boldsymbol{\sigma} + \boldsymbol{d}^{T\alpha} \cdot \vec{E})\xi^\alpha \tag{35}$$

$$\vec{P}^g = \sum_{\alpha=1}^{6} (\vec{P}_0^{\alpha} + \boldsymbol{d}^{\alpha} : \boldsymbol{\sigma} + \boldsymbol{\kappa}^{\alpha} \cdot \vec{E}) \xi^{\alpha} \tag{36}$$

The response of all grains in local coordinate system is transformed into global coordinate system using transformation laws. At the end of each loading step, the volume fractions of the domains are updated. The macroscopic material behavior is obtained by averaging the response of all the grains, i.e., the macroscopic strain, $\boldsymbol{\varepsilon}$, is obtained as the average of strains of all the individual grains, $\boldsymbol{\varepsilon}^g$, while the macroscopic polarization, $\vec{P}$, is obtained as the average of polarizations of all the individual grains, $\vec{P}^g$.

6 Results and discussions

Initially, to test the suitability of the developed model, it was applied on a single crystal ferroelectric to predict its response under different loading conditions with the influence of constrained boundary. Experiments conducted on a single crystal barium titanate under constrained boundary offered by a loading platen were considered for simulations (Burcsu, Ravichandran, and Bhattacharya (2004)). Keeping the magnitude of compressive stresses constant at 0, 0.36, 0.72 and 1.07 MPa, the electric field was varied to obtain the behavior of single crystal barium titanate. The simulated response using the proposed model was compared with the experimental results. The material parameters used in the simulations were obtained from literature (Burcsu, Ravichandran, and Bhattacharya (2004); Shilo, Burcsu, Ravichandran, and Bhattacharya (2007)). In the experiment, actuation strain was used to plot the graphs, which is the difference between the maximum and minimum strains. In accordance with that, the actuation strain was used here in plotting graphs for single crystal barium titanate. Material constants K_1 and K_2 were obtained by fitting the simulations on experimental graphs at a particular constant compressive stress and varying electric fields. With these values of the material constants, polarization vs. electric field and strain vs. electric field graphs were plotted for other loading conditions as shown in Fig.2 and Fig.3. The simulations are found to be comparable with the experimental results with respect to the magnitudes of the strain and the polarization. The fact that the crystal undergoes only 180^0 switching under pure electric loading is realized by the horizontal line obtained in strain vs. electric field plot (Fig.2). With increase in compressive stress, 180^0 switching occurs through two consecutive 90^0 switching and this gives rise to the actuation strain.

The model was then applied to a polycrystalline ferroelectric to predict its response under variety of loading conditions. The results of various experiments reported in literature (Fang and Li (1999)), conducted on a soft PZT under electrical, mechanical and electro-mechanical loading conditions are used for comparison with the proposed model predictions. The appropriate material properties of soft PZT were obtained from the literature (Lu, Fang, Li, and Hwang (1999)). The materials constants K_1 and K_2 were determined by correlating simulations with experimental curves for a certain set of electro-mechanical loading conditions.

In the absence of electric field, i.e., in ferroelastic case, the response of PZT was predicted and compared with the experimental results in terms of stress vs. strain and stress vs. electric displacement as shown in Fig.4. In the experiment conducted by Fang and Lu (1999), the PZT was fully poled along positive x_3 axis with the help of external electric field. Then, the compressive stress was applied gradually along x_3 axis, parallel to the poled direction of ferroelectric. This caused 90^0 switching from positive x_3 axis to any of the four directions that are normal to x_3 axis, i.e., positive and negative axes of x_1 and x_2, in such a way that their average polarization is almost zero. Hence, at the end of the loading, the material reached a mechanically depoled state, where, the net polarization became zero and the strain along x_1 and x_2 axis were found to be about half of the strain along x_3 axis. The simulated response in Fig.4 indicate a good match with the experimental results.

Under electromechanical loading, the electric field was varied with constant compressive stresses at -20, -40 and -60 MPa respectively. The predicted response and the experimental results are compared in terms of polarization vs. elec-

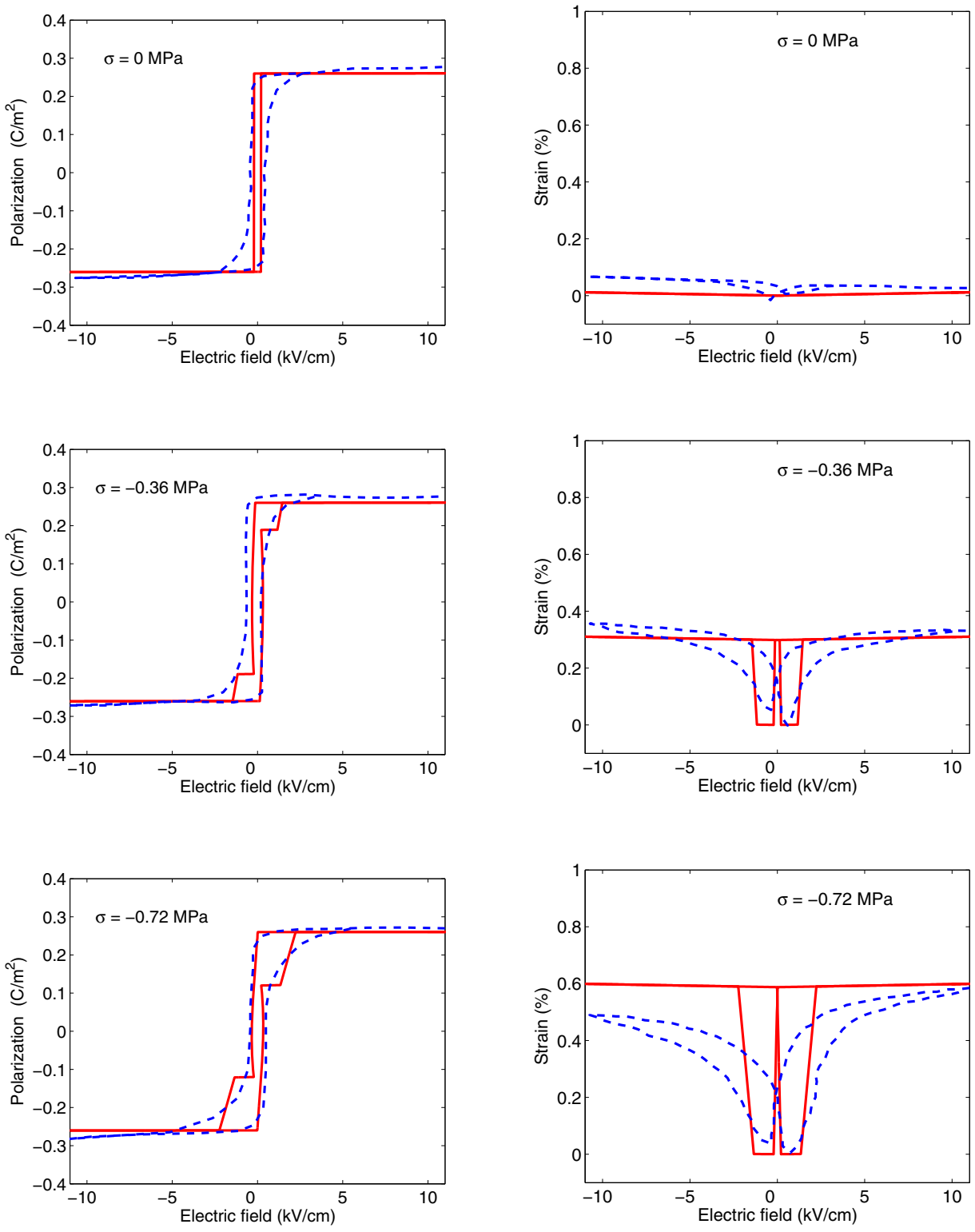

Figure 2: Hysteresis (left) and butterfly (right) curves of single crystal $BaTiO_3$ under electromechanical loading with axial compressive stresses, $\boldsymbol{\sigma} = 0, -0.36, -0.72$ MPa; Solid-simulated, dashed-experiment (Burcsu, Ravichandran, and Bhattacharya (2004))

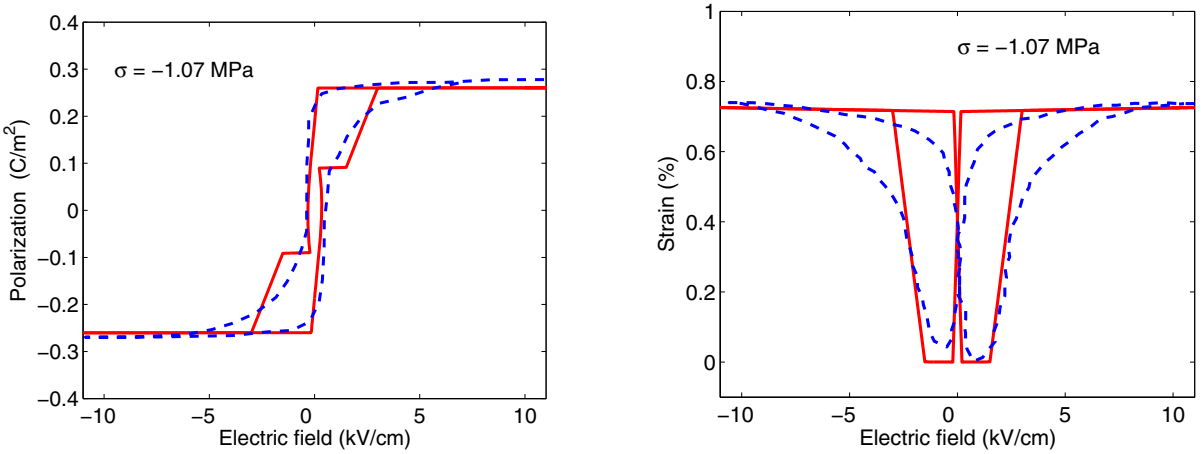

Figure 3: Hysteresis (left) and butterfly (right) curves of single crystal $BaTiO_3$ under electromechanical loading with axial compressive stress, $\boldsymbol{\sigma} = -1.07$ MPa; Solid-simulated, dashed-experiment (Burcsu, Ravichandran, and Bhattacharya (2004))

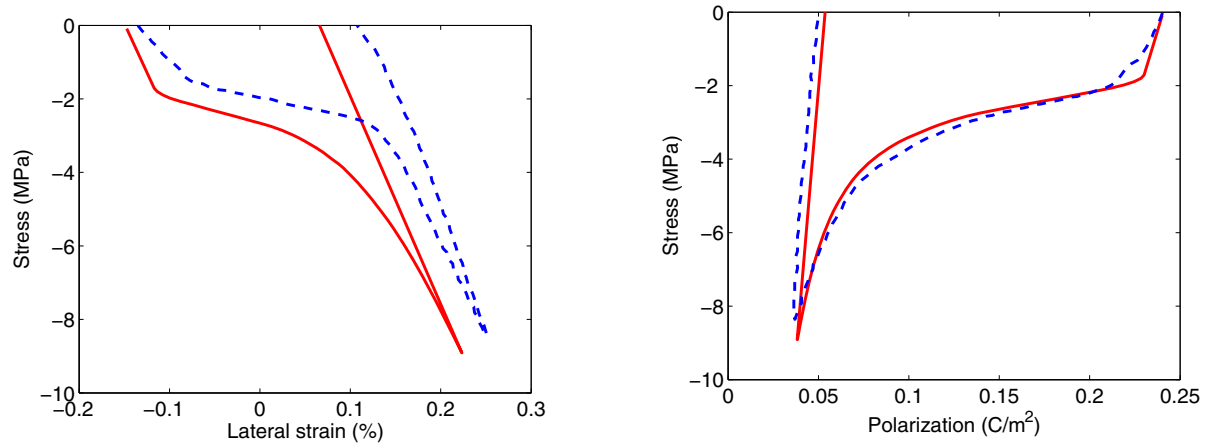

Figure 4: Stress vs. strain (left) and stress vs. polarization (right) curves of polycrystal PZT under mechanical loading; Solid-simulated, dashed-experiment (Fang and Li (1999))

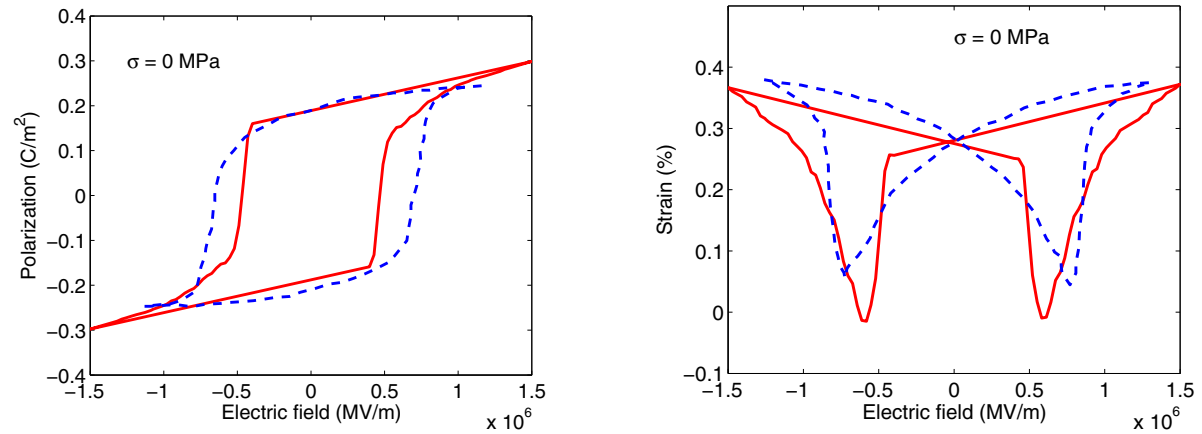

Figure 5: Hysteresis (left) and butterfly (right) curves of polycrystal PZT under electromechanical loading with axial compressive stress, $\boldsymbol{\sigma} = 0$ MPa; Solid-simulated, dashed-experiment (Fang and Li (1999))

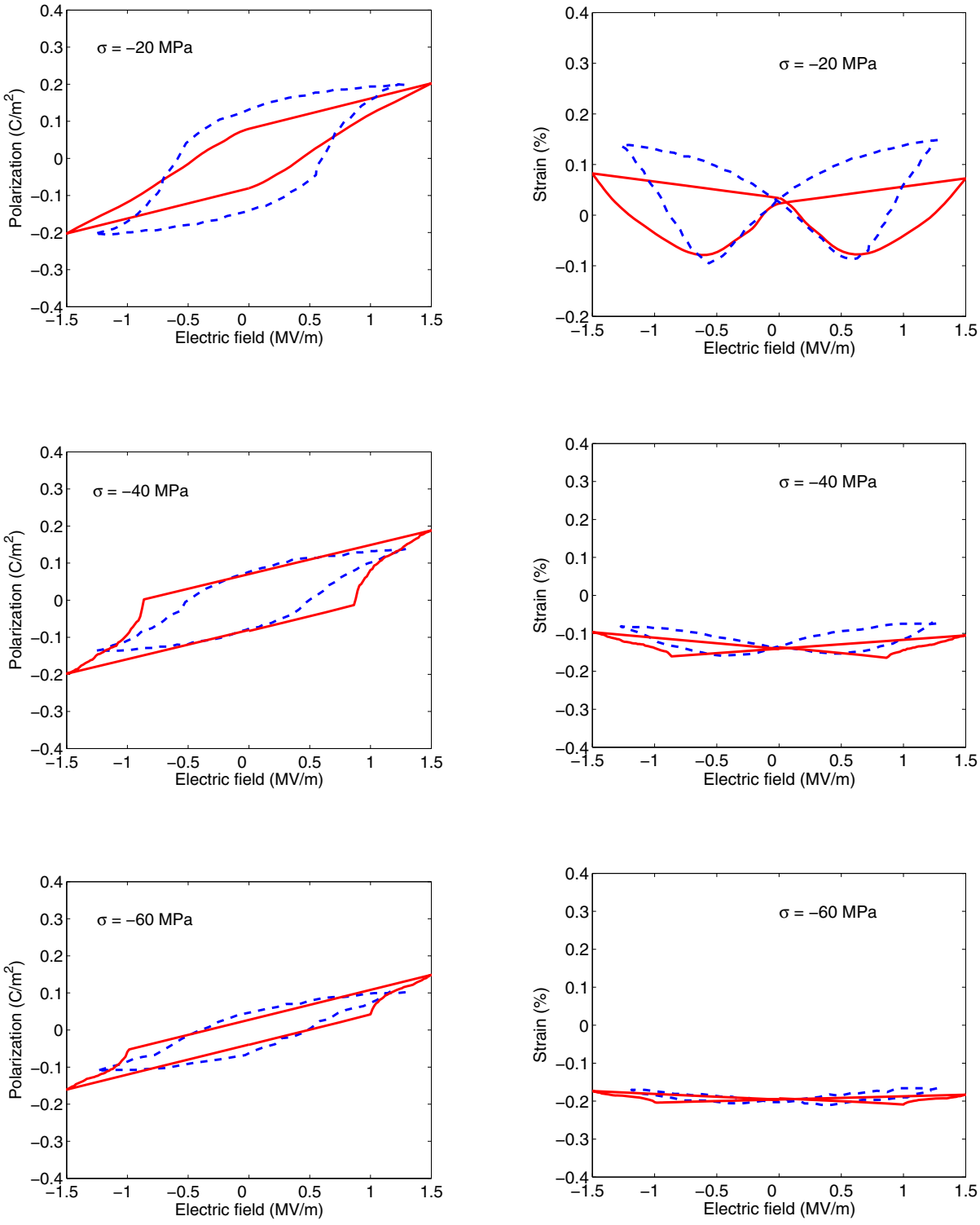

Figure 6: Hysteresis (left) and butterfly (right) curves of polycrystal *PZT* under electromechanical loading with axial compressive stresses, $\boldsymbol{\sigma} = -20, -40, -60$ MPa; Solid-simulated, dashed-experiment (Fang and Li (1999))

tric field and strain vs. electric field in Figs. 5 and 6. As the compressive stress magnitude increases, the classic butterfly curve in strain-electric field plot gets compressed and moves downwards which is clearly captured by the proposed model. The contraction in polarization-electric field plot has also clearly reflected in the model predictions. These are due to the increasing resistance to 90^0 switching in the direction parallel to the applied stress.

The significance of introducing grain boundary resistance in the proposed model was verified by plotting the graphs with and without the resistance in the model. The simulated strain without including additional resistance was found to be much higher than the experimental strain in the single ferroelectric, justifying the need for the introduction of boundary effects related additional resistance. Besides, to support the contention that the grain boundary resistance is predominantly due to 90^0 switching, 180^0 switching was also assumed to experience the boundary resistance in addition to 90^0 switching and the simulations were performed. No appreciable difference was observed. This may be attributed to a weaker resistance due to the electrical boundary effects compared to the resistance due to the strain related boundary effects.

7 Conclusions

In this work, a three dimensional micromechanical model for ferroelectrics has been developed based on firm thermodynamics basis. The dissipative mechanisms in the subgrain of a ferroelectric polycrystal, due to the resistance offered at its boundary by the adjacent grains during domain switching are identified and the dissipation thresholds have been appropriately refined. The consideration of the additional dependence of the dissipation threshold on the applied stress corroborates well with experimental results under compressive loading conditions confirming the influence of resistance role played by the grain boundary. Thus, backed by a physical motivation, a firm thermodynamic basis and representative example simulations, the model has the ability to include dissipative grain boundary effects under combined electromechanical loadings in the simulation of polycrystal ferroelectric behavior and, at the same time, preserve the computational advantages. Since, the grain boundary size could play a major role in the resistance, it is likely that size effects may be observed in the polycrystal ferroelectrics. It remains to be confirmed from the future experiments on polycrystals with different grain sizes whether such a size effect is observed.

References

Arockiarajan, A.; Menzel, A. (2007): On the modeling of rate-dependent domain switching in piezoelectric materials under superimposed stresses. *CMES: Computer Modeling in Engineering & Sciences*, vol. 20, pp. 55–72.

Arockiarajan, A.; Menzel, A.; Delibas, B.; Seemann, W. (2006): Micromechanical modeling of switching effects in piezoelectric materials - a robust coupled finite element approach. *Euro. J. Mech. A/Solids*, vol. 25, pp. 950–964.

Burcsu, E.; Ravichandran, G.; Bhattacharya, K. (2004): Large electrostrictive actuation of barium titanate single crystals. *J. Mech. Phys. Solids*, vol. 52, pp. 823–846.

Chen, W.; Lynch, C. S. (1998): A micro-electro-mechanical model for polarization switching of ferroelectric materials. *Acta Mater.*, vol. 46, pp. 5303–5311.

Cocks, A. C. F.; McMeeking, R. M. (1999): A phenomenological constitutive law for the behavior of ferroelectric ceramics. *Ferroelectrics*, vol. 228, pp. 219–228.

Fang, D.; Li, C. (1999): Nonlinear electromechanical behavior of a soft pzt-51 ferroelectric ceramic. *J. Mat. Sci.*, vol. 34, pp. 4001–4010.

Huber, J. E. (2005): Micromechanical modeling of ferroelectrics. *Current opinion solid state Mat. Sc.*, vol. 9, pp. 100–106.

Huber, J. E.; Fleck, N. A.; Landis, C. M.; McMeeking, R. M. (1999): A constitutive

model for ferroelectric polycrystals. *J. Mech. Phys. Solids*, vol. 47, pp. 1663–1697.

Hwang, S. C.; Huber, J. E.; McMeeking, R. M.; Fleck, N. A. (1998): The simulation of switching in polycrystalline ferroelectric ceramics. *J. Appl. Phys.*, vol. 84, pp. 1530–1540.

Hwang, S. C.; Lynch, C. S.; McMeeking, R. M. (1995): Ferroelectric/ferroelastic interactions and a polarization switching model. *Acta Metall. Mater.*, vol. 43, pp. 2073–2084.

Hwang, S. C.; McMeeking, R. M. (2000): A finite element model of ferroelectric / ferroelastic polycrystals. *Proc. SPIE.*, vol. 3992, pp. 404–417.

Kamlah, M. (2001): Ferroelectric and ferroelastic piezoceramics - modeling and electromechanical hysteresis phenomena. *Continuum Mech. Thermodyn.*, vol. 13, pp. 219–268.

Kamlah, M.; Jiang, Q. (1999): A constitutive model for ferroelectric pzt ceramics under uniaxial loading. *Smart Mat. Struct.*, vol. 8, pp. 441–459.

Landis, C. M. (2004): Non-linear constitutive modeling of ferroelectrics. *Current opinion solid state Mat. Sc.*, vol. 8, pp. 59–69.

Landis, C. M.; McMeeking, R. M. (2000): A phenomenological constitutive law for ferroelastic switching and a resulting asymptotic crack tip solution. *J. Intelligent Mat. Sys. Struct.*, vol. 10, pp. 155–163.

Lu, W.; Fang, D. N.; Li, C. Q.; Hwang, K. C. (1999): Nonlinear electric-mechanical behaviour and micromechanics modeling of ferroelectric domain evolution. *Acta Mater.*, vol. 47, pp. 2913–2926.

McMeeking, R. M.; Landis, C. M. (2002): A phenomenological multiaxial constitutive law for switching in polycrystalline ferroelectric ceramics. *Int. J. Engng. Sci.*, vol. 40, pp. 1553–1577.

Michelitsch, T.; Kreher, W. S. (1998): A simple model for the nonlinear material behavior of ferroelectrics. *Acta Mater.*, vol. 46, pp. 5085–5094.

Shaikh, M. G.; Phanish, S.; Sivakumar, S. M. (2006): Domain switching criteria for ferroelectrics. *Comput. Mater. Sci.*, vol. 37, pp. 178–186.

Shieh, J.; Huber, J. E.; Fleck, N. A. (2003): An evaluation of switching criteria for ferroelectrics under stress and electric field. *Acta Mater.*, vol. 51, pp. 6123–6137.

Shilo, D.; Burcsu, E.; Ravichandran, G.; Bhattacharya, K. (2007): A model for large electrostrictive actuation in ferroelectric single crystals. *Int. J. Solids Struct.*, vol. 44, pp. 2053–2065.

Sun, C. T.; Achuthan, A. (2001): Domain switching criteria for piezoelectric materials. *Proc. SPIE.*, vol. 4333, pp. 240–249.

Sun, C. T.; Jiang, L. Z. (1998): Domain switching induced stress at the tip of a crack in piezoceramics. *Proc. 4th ESSM 2nd MIMR*, pp. 715–722.